Specific criteria used to identify possible pyroclastic deposits included the presence of an irregular central depression, an albedo anomaly with diffuse boundaries, and a distinct spectral signature similar to that of the previously identified pyroclastic deposit RS-03. These criteria are similar to those used to identify lunar pyroclastic deposits, though lunar deposits are also distinguished by their low albedo compared with surrounding terrain (Pieters et al., 1974; Weitz et al., 1998; Gaddis et al., 2003), whereas mercurian pyroclastic deposits tend to have a higher albedo than surrounding terrain.

On the basis of these criteria, a total of 35 candidate pyroclastic deposits have been identified on Mercury, including 19 newly documented deposits and multiple distinct deposits at some of the previously identified sites (Fig. 2, Table 1). Most of the pyroclastic deposits so identified fit all three criteria, though several large deposits lack a discernible central vent, and several deposits are located in the areas for which sufficient WAC color data are not yet available. The Beckett crater deposit is an example of a feature with good lighting for morphological analysis but poor lighting geometry for spectral analysis, whereas the Melville, Hemingway, and RS-04 deposits are examples of features with good lighting geometry for spectral analysis but poor lighting for morphological analysis (Fig. 2). The additional candidate pyroclastic deposits identified from images obtained during the second and third flybys are generally located on the floors of impact craters, though some are located along crater peak rings, and one (Melville) is located just outside the rim of a crater (Table 1).

Note added in proof: Four additional pyroclastic deposits were identified after this manuscript was submitted. These four features, which bring the total number of candidate pyroclastic deposits to 39, are included in Figs. 1 and 2 and Table 1 (labeled Penta and unnamed crater 5a–c, after the areas in which they are found) but are not included in the analyses that follow.

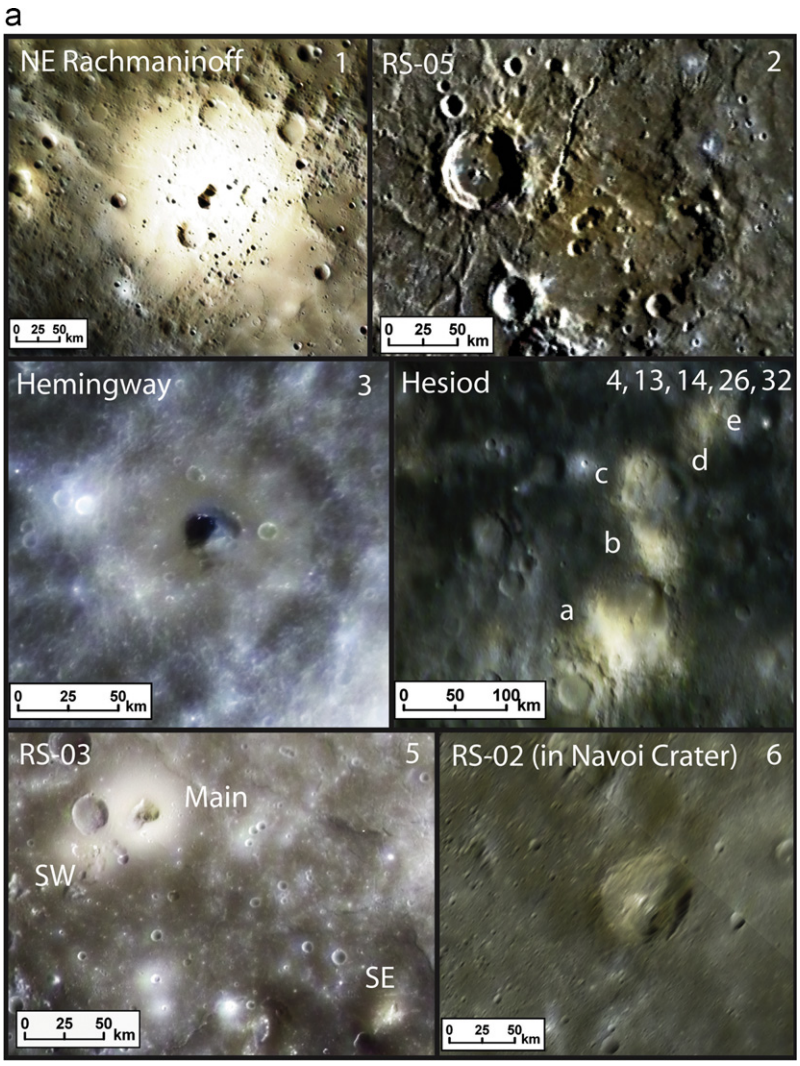

Fig. 2. Candidate pyroclastic deposits identified from images obtained during the three MESSENGER flybys. Higher-resolution images were taken from a global mosaic of Mercury combining MDIS NAC data with images from Mariner 10 (Becker et al., 2009) and overlaid with color images from a global WAC mosaic (Domingue et al., 2010) (R: 1000 nm, G: 750 nm, B: 430 nm). Numbers correspond to the position of each deposit in Table 1 (with 1 the largest and 35 the smallest). The WAC data were overlaid on the NAC data using an Adobe Photoshop blending filter that highlights WAC color variations while preserving NAC contrast and texture, effectively reducing the appearance of WAC pixels. Most deposits have diffuse edges and a distinguishable color anomaly and are centered on an irregular depression. (a) Some large deposits such as Hemingway (3) and Hesiod a (4) do not have clear vents. Deposit RS-05 has several possible vent structures. RS-02 (located in the crater Navoi, 6) lies in an area with poor viewing geometry (Fig. 1c). (b) To Ngoc Van (10), Scarlatti (12), and Gibran (15) were identified as pit craters by Gillis-Davis et al. (2009). The To Ngoc Van deposit (10) lies in an area imaged at poor viewing geometry (Fig. 1). (c) Rachmaninoff SE (17), RS-04b and c (20 and 23), and RS-01 (located in the crater Moody, 25) lack discernible vents. RS-04 is located in an area of high illumination angle, making morphological features more difficult to discern (Fig. 1c). (d) Deposits Beckett (34), Glinka (29), and unnamed crater 4 (not measured) lie at the edges of the WAC image data in the areas of high illumination angle.